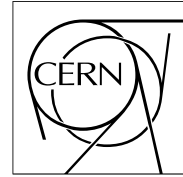


The Compact Muon Solenoid Experiment

CMS Note

Mailing address: CMS CERN, CH-1211 GENEVA 23, Switzerland



November 9, 2006

Predicting the Gain Spread of the CMS Tracker Analog Readout Optical Links

Stefanos Dris^{1,2}, Karl Gill², Jan Troska², Francois Vasey²

¹*Imperial College, London, UK*

²*CERN, Geneva, Switzerland*

Abstract

Approximately 40 000 analog optical links will read out the data from 10 million silicon microstrips in the CMS Tracker. In an analog system, the overall gain directly determines the dynamic range and resolution of the data being read out. There is a sufficiently large amount of production data available to allow the extraction of the real distribution of gain for each component making up the complete optical link. The purpose of this study is to examine the aggregate effect of the individual component gain distributions on the readout system's dynamic range, and its uniformity throughout the thousands of deployed links in the CMS Tracker. To this end, a Monte Carlo simulation based on production test data, and augmented with results from deployed links in real test systems, has been carried out. The results give an estimate of the spread in gain and dynamic range that can be expected in the final system, running at -10°C .

1. Introduction

The CMS Tracker [1] comprises ~ 10 million silicon microstrips that generate data read out by $\sim 40\,000$ analog optical links. Inside the Tracker volume, signals from the microstrips are sampled by APV25 [2] readout chips at the LHC bunch crossing frequency of 40MHz. On receipt of a trigger, the data from 256 microstrips (2 APVs) are time-multiplexed and formatted into a frame that is then transmitted ~ 65 m to the counting room via analog optical links. Digitization of the data is performed by Front End Driver (FED) VME cards [3] situated in the counting room, before being sent on to the data acquisition (DAQ) system.

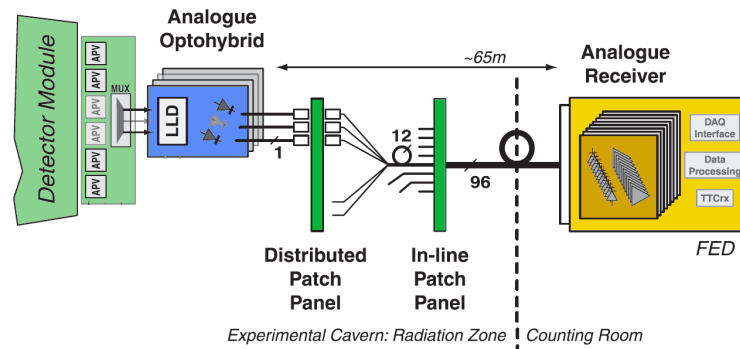


Figure 1: The analog readout optical link.

Optical fiber is an ideal medium for such a transmission system, due to its immunity to electromagnetic interference (EMI), potential for low power dissipation and low mass. The sheer number of channels required to be read out in the CMS Tracker make the use of copper transmission prohibitive. An analog system was preferred in order to eliminate the need for digitization on the detector hybrids, thereby simplifying the front end electronics and lowering power consumption inside the Tracker volume. In addition, all of the information from the detectors is preserved and sent to the counting room where the data can be manipulated on the FED (e.g., zero-suppressed) as dictated by the final operating environment.

The analog readout link is shown in Figure 1. The light from a single-mode, 1310nm wavelength, edge-emitting laser is amplitude modulated by the Linear Laser Driver (LLD) ASIC [4] on the Analog OptoHybrid (AOH) [5]. The LLD was designed with four gain settings, allowing a certain amount of gain equalization in the final system. This also allows for compensation due to radiation damage: It has been shown that laser efficiency will drop by up to $\sim 5\%$ in the worst case [6], while the loss resulting from radiation damage in the optical fiber will be of the order of 0.4-0.6dB [7]. Each AOH contains either 2 or 3 pigtailed lasers connected via single-way MU-type connectors to a 12:1 fan-in (the Distributed Patch Panel) at the periphery of the Tracker. The fan-in merges 12 single fibers into a 12-fiber ribbon. A transition to a rugged, multi-ribbon cable is made at the In-line Patch Panel via 12-channel MFS type connectors. The ruggedized cable carries 8 ribbons to the counting room, each of which connects directly via MPO12 connectors to one of the 12-channel Analog Optoelectronic Receivers (ARx12) [8] mounted on FEDs.

One of the most important parameters in an analog readout system is the gain, which directly affects the size and resolution of detector signals that can be captured at the output of the link. The overall link gain is determined by the aggregate effect of all constituent components. The work presented in this document will determine the distribution of gains that can be expected in the final CMS Tracker readout system, and its effect on the dynamic range is explored.

The present study is an extension of the work presented in [9], where the distributions of the individual component gains were assumed to be uniform within their specifications. The previous study was essentially a ‘worst-case scenario’ as far as the total gain spread is concerned. The main difference in the current study is that quality assurance data from production testing is used to compile histograms of the gain for each component. A Monte Carlo simulation that samples the real data is used to produce the most realistic prediction for the link gain spread to date.

Section 1.1 gives an overview of the setup routine used for calculating the optical link gain. A brief description is necessary for understanding the subsequent results.

Section 2 reviews the work presented at the 10th Workshop on Electronics for LHC and Future Experiments [10] which constituted the first use of component production test data to predict the final system gain spread by simulation. Since production tests take place at room temperature, the first iteration of the simulation could only be used for predicting the gain spread at room temperature. The results obtained via simulation are compared to those from a deployed TEC system in the May 2004 test beam [11].

Section 3 details the gain spread observed in optical links deployed in test beam systems, comprising the full readout chain components. The results from the October 2004 test beam using the Tracker Outer Barrel (TOB) Cosmic Rack (CRack) [12] were used to establish the variation of gain with temperature. This was facilitated by the presence of a cooling system in the CRack with the ability to operate at sub-zero temperatures. The accuracy of the gain calculation method is validated using physics data from the test beam.

Having calculated the average variation of link gain with temperature, the simulation of optical link gains has been updated and the results appropriately scaled to give the final prediction of dynamic range spread for the nominal Tracker operating temperature. The results are detailed in section 4.

1.1 Principle of the Gain Calculation Method

Figure 2 is an example of the data transmitted by the readout links. The detector signals are sampled and transmitted in analog form by the optical links. They are encapsulated in a frame also containing digital data; a digital header (3 bits, all logic ‘1’) followed by the APV pipeline address used to store the analog data, and an error bit [2]. A stop bit is added after the analog data. At the output of the APV, the height of the digital header is nominally $\pm 4\text{mA}$. This translates to $\pm 400\text{mV}$ (or 800mV differential) at the input to the AOH. At the nominal APV gain of 1MIP/mA for thin ($320\mu\text{m}$) detectors, the digital header is

equivalent to an 8MIP signal. In this document it is assumed that the APV digital header height is constant. In practice there is a variation from chip to chip of $\sim 5\%$, as demonstrated in [13, 14]¹.

It is important to note that the digital header height is not affected by any of the APV's settings. It is thus a constant for the duration of CMS operation, relative to other parameters in the front-end electronics. The optical link setup routine makes use of this quantity for calculating the link gain (and hence picking the appropriate AOH gain setting). This is essentially an approximation of the real 'particle gain', which is the quantity which is of most importance to the Tracker readout system. The term 'particle gain' refers to the amplification (or attenuation) of the signals arising from particles traversing the detectors.

Furthermore, it is worth noting that the APV tick height (800mV) exceeds the specification for optical link linearity of 600mV (differential). Hence, it could be expected that signal compression in the link would compromise the accuracy of any technique based on measurements of APV tick height. The relationship between the particle gain and that calculated from the setup routine is briefly introduced in section 3.1. There is no evidence of non-linear degradation in the results obtained.

During an optical link setup run (often referred to as 'gain scan'), the APV outputs synchronization pulses (or 'ticks') [2]. These are identical in height to the digital header. The FED captures the transmitted APV ticks and the height of the tick is measured. Based on the assumption that the tick height is 800mV at the input of the link, and given that each FED ADC count corresponds to 1mV, the overall readout link gain in V/V is determined by simply dividing the output height in ADC counts by 800.

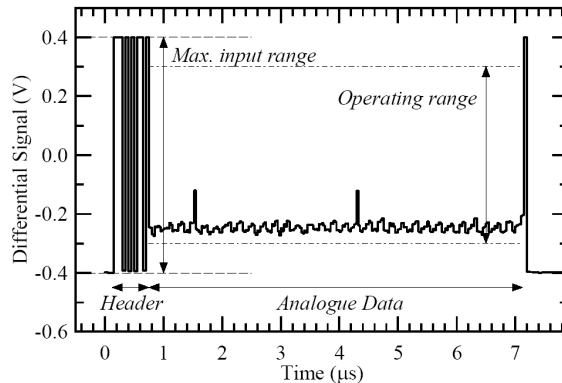


Figure 2: Typical data frame at the input of the readout link. The analog data are time multiplexed at a ratio of 256:1 with a sample-width of 25ns.

¹ The absolute value of the digital header height is not known in FED ADC counts [ref], and is assumed to be $\pm 400\text{mV}$ at the input of the optical link.

2. Predicted Optical Link Gain Distribution from Production Data

The optical links made up of electronic, optoelectronic and optical components must match the performance requirements of the overall readout system in terms of dynamic range and resolution. The readout links are required to transmit 3.2MIPs with 8bit resolution¹ [9]. A statistically significant set of test data allows the extraction of real distributions of the components' performance parameters. The distributions used are shown in Figure 3. The overall link gain spread is determined by the aggregate effect of all constituent components' gain distributions.

A Monte Carlo simulation has been produced to compute the complete link gain distribution from the available component production test data. On the transmitting side, the LLD on the AOH was designed with switchable gain settings to compensate for component gain tolerances. Four gain settings are available, with nominal values of 5.0, 7.5, 10.0 and 12.5mS, allowing a certain amount of gain equalization in the final system. The effect of switching on the gain distribution is investigated. The results obtained are detailed in [10], but will be reviewed in this section, along with the method followed.

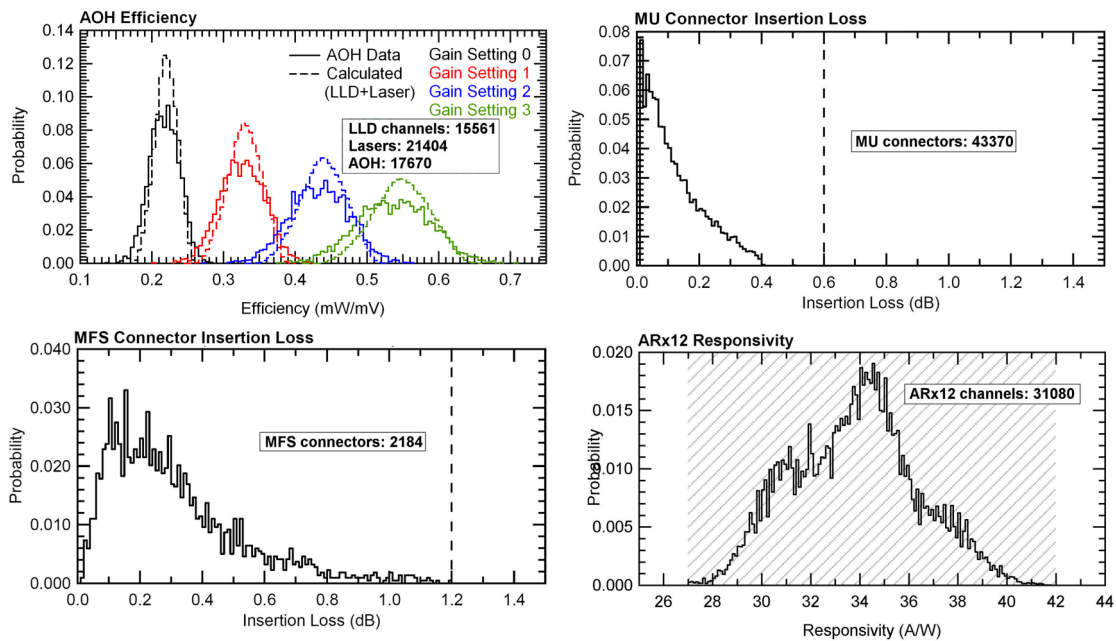


Figure 3: PDFs of the component gains used in the Monte Carlo simulation. Shaded areas and dotted lines indicate specification limits. The number of channels used in each case is also indicated.

2.1 Simulation Method and Room Temperature Results

The simulation model includes the gain spreads of all optical link components, including the insertion loss of the connectors at each patch panel (Figure 4). The ARx12 output resistor value is assumed to be 100 Ω

¹ For 320 μ m silicon strip detectors.

for this simulation. The inverse transform method [15] is used to sample the gain distributions –or probability density functions (PDF)– of each of the components¹. In each iteration of the Monte Carlo simulation, the samples are multiplied together to obtain four overall link gains, each one corresponding to one of the four AOH (LLD) gain settings. The simulation can be run using equalization (i.e. selecting one of the four gains that is closest to the nominal target gain of 0.8V/V) or by simply selecting the gain corresponding to the same AOH setting for every link. The process is illustrated in the flow chart of Figure 5.

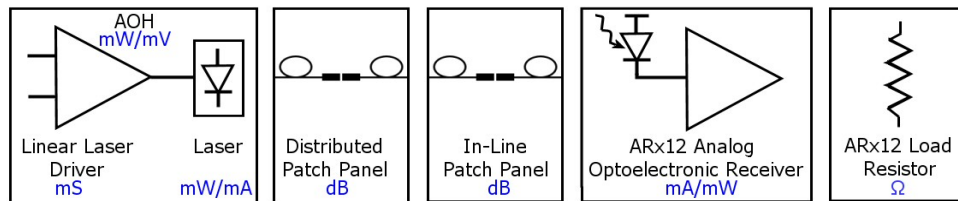


Figure 4: Optical link components used in the Monte Carlo simulation.

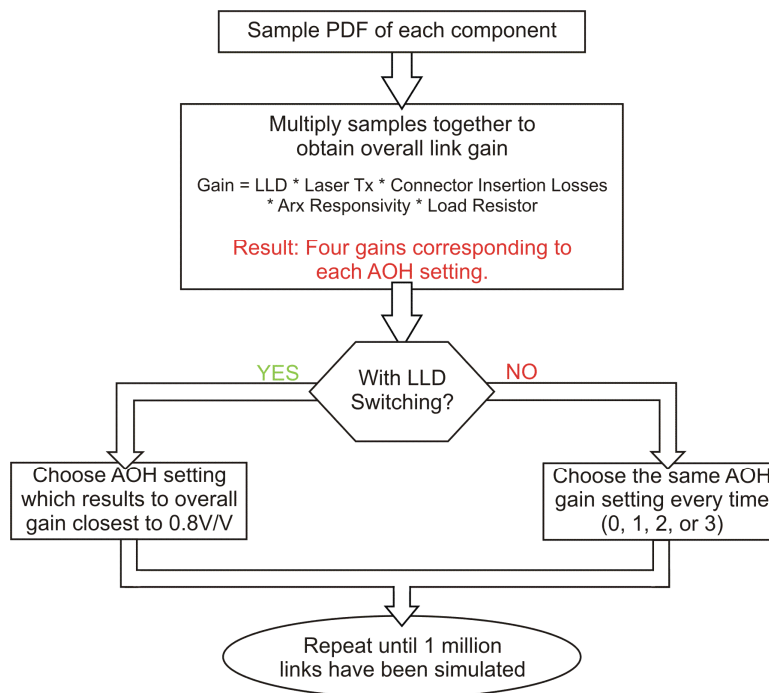


Figure 5: Flow chart for the Monte Carlo simulation of optical link gain.

The simulation was first run for each of the four gain settings of the LLD, without any attempt at equalization. The resulting distributions are roughly Gaussian (Figure 6). The nominal gain of 0.8V/V is

¹ The gain spreads of the APV, APVMUX and the FED’s analog front-end electronics (except the ARx12 load resistor) are not taken into account in this study.

also shown on the plot (dashed line). There is a very large gain accessible range using the available LLD settings. The position of the distributions with respect to the 0.8V/V specification suggests that lower gain links can be better compensated by using higher gain settings. The high-end tail of the gain 0 trace exceeds the nominal gain, and since these links are already at their lowest setting, they cannot be further compensated. Figure 6 also shows the relationship between the link gain in V/V and the height of the APV tick in FED ADC counts. The scale assumes that an APV tick is 800mV at the input of the AOH (or 8mA output from the APV), and that the gain of the FED ADC is 1 ADC count/mV [3].

The simulation was also run incorporating the ability to switch between LLD settings in order to equalize all gains as close as possible to the nominal value. Figure 7 shows the resulting spread. The laser driver switching process can be thought of as cutting into the source distributions (i.e. the single-gain distributions of Figure 6) and selecting the slices centered on 0.8V/V. This is best visualized in Figure 6, where the switched spread is superimposed on the ‘single-gain’ distributions (shaded area). Figure 7 shows the switched gain in more detail. The distribution has two distinct boundaries equidistant from the target gain value, with the lower limit at ~0.64V/V, and the upper limit at ~0.96V/V.

It should be noted that there are very few links (0.007% of the 1 million simulated links) that lie above the upper limit in the switched gain distribution, and are not visible in the plot. This is due to the tail of the Gain 0 distribution that exceeds the limit of 0.96V/V. These links are already at their lowest gain setting, and cannot be further compensated. Clearly, it is not an ideal situation to have any part of the Gain 0 distribution above the upper limit.

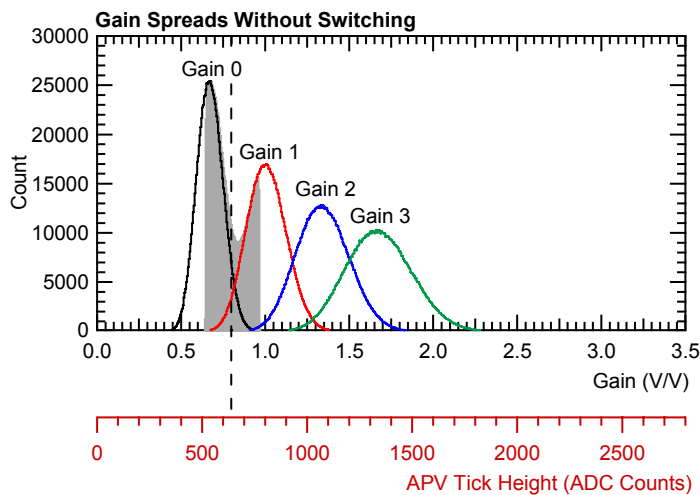


Figure 6: Showing the ‘single gain’ spread distributions predicted by simulation using real production data without switching of the LLD. The shaded area shows the distribution resulting after equalization using the four available gain settings.

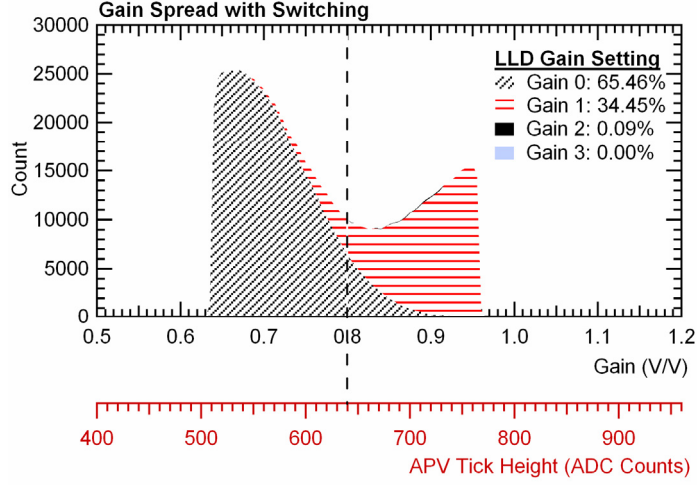


Figure 7: Equalized link gain distribution obtained by switching of the LLD, showing the contributions from each gain setting.

The maximum spread of the equalized gain distribution can be determined analytically given the simple switching algorithm that selects the gain closest to the target value. For the following analysis the upper extent of the equalized distribution is denoted by u , while the lower limit is l (in V/V). We begin by imposing the restriction that the high-end tail of the gain 0 distribution (see Figure 6) must be lower than u and the low-end tail of the gain 3 distribution must be above l . In addition, we will assume that the dominant gain settings used when equalizing are settings 0 and 1, since this gives the maximum spread (this will occur when equalization around the target gain is achieved by using mostly these two settings). Since the equalization algorithm selects the gain closest to the target value of 0.8V/V , it follows that the extents of the equalized distribution will be equidistant from the target:

$$\begin{aligned} 0.8 - l &= u - 0.8 \\ \Rightarrow u + l &= 1.6 \end{aligned} \quad (1)$$

The resolution of the gain settings determines the worst-case difference between the lowest and highest equalized link gains. From production test data of the LLD chip [10] it is known that the four available gain settings are (on average) 5.38, 8.06, 10.74 and 13.41mS (see Figure 8). Hence, the maximum ratio of successive gain settings occurs between gain setting 0 and gain setting 1, and is 1.5 ($8.06/5.38 \sim 1.5$). Any link that has a gain less than l clearly will have to be set to the next highest gain setting to achieve a gain closer to 0.8V/V . Similarly, any gain over u must be set to the next lowest gain setting. This implies that, at worst, the relationship between u and l is given by:

$$u = 1.5l \quad (2)$$

Solving for u and l ,

$$l = 0.64 \text{ and } u = 0.96 \text{ (V/V)} \quad (3)$$

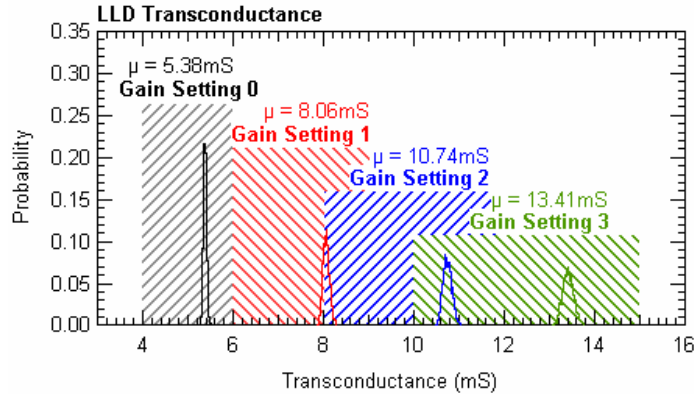


Figure 8: PDFs of Linear Laser Driver transconductance for each of the four gain settings selectable on the AOH. Shaded areas indicate the corresponding specification boundaries

Having established the gain distribution, the spread in dynamic range can be determined. The impact of the switched link gain spread on the dynamic range of the readout system is illustrated in Figure 9. After the analog signals are transmitted through the optical links, they undergo digitization by a 10-bit, 1.024V input-range ADC [3] on the FED in the counting room. Digitization and processing (including pedestal subtraction) is performed, and the two MSBs of the data are discarded¹. It is therefore useful to look at the signal size that can be transmitted by the system using 8 bits, before clipping occurs. The signal size is in terms of electrons and is easily related to MIPs for both thin and thick detectors. Hence the dynamic range figure of merit can be expressed in electrons/8bits or MIPs/8bits².

The dynamic range spread can be determined from Figure 9, where the signal size at the link's output (in ADC bits) is plotted against the signal size at the link's input (in electrons and MIPs). By interpolation, it is possible to determine the signal sizes that can be accommodated in 8bits of the FED's ADC (horizontal dotted line). Hence, at the specified gain, signal sizes up to 80 000 electrons (3.2 MIPs) can be transmitted in their entirety. The shaded area around this line corresponds to the full range of gains predicted by the simulation, using equalization. Again, by interpolation, the maximum signals that fit in 8bits will range from ~66 000 to 100 500 electrons.

On the same figure, the spread in dynamic range (in electrons/8bits and MIPs/8bits) is also shown in the form of a histogram. There are a few statistically insignificant links (0.007%) with a dynamic range between 63 200 and 66 500 electrons/8bits. These are the same simulated links having gains over 0.96V/V in the switched gain spread (Figure 7). Ignoring these, the dynamic range of the links will lie between 66 500 and 100 500 electrons/8bits.

¹ This is the case in the current FED firmware; in the future it may be possible for the users to select which data bits they wish to retain in the captured data.

² Note that these two quantities depend on the detector thickness. This is reflected in the additional axes of Figure 9, where (an approximate) relation between signal size in electrons and MIPs for thin and thick detectors is given.

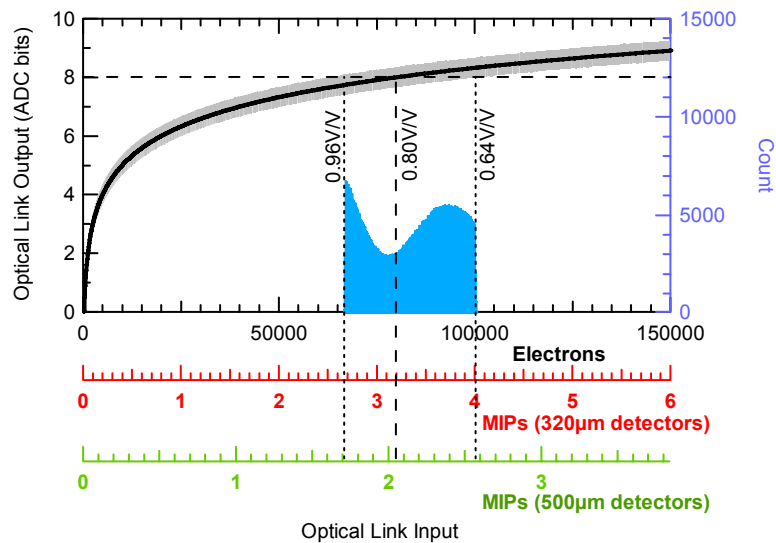


Figure 9: Showing Optical Link Output vs Input in ADC bits (left axis). The histogram (right axis) shows the spread in dynamic range.

The signal sizes can also be interpreted in MIPs, assuming that 1 MIP produces 25 000 electrons in thin detectors, and 39 000 in thick detectors (see bottom axes of Figure 9). For thin detectors, the maximum signal sizes will be between 2.65 and 4 MIPs/8bits. The corresponding range for thick detectors is 1.7 to 2.6 MIPs/8bits.

2.2 Comparison to the Gain Spread from Deployed Optical Links at Room Temperature

The gains of real optical links deployed in the May 2004 test beam by the Tracker End Cap (TEC) subsystem [11] were compared to the results obtained by simulation. The TEC system link gains were calculated using the data obtained by the automated setup runs.

The gains of 121 TEC optical links with no cooling were determined and histograms obtained for each AOH gain setting. Figure 10 shows the single-gain distributions obtained by simulation (dotted lines) and the Gaussian fits to the histogrammed data from the TEC system (solid lines). It is immediately obvious that the real system gains are slightly higher: The mean of the simulated gain 0 distribution is 0.67, compared to 0.69 from the TEC data. In addition, the spread is higher in the real links (standard deviation=0.15 versus 0.10). This is not surprising, given that there are components of the readout chain that have not been simulated (e.g. APV25 and APVMUX chips, as well as passive and active components on the Front End Driver board (FED) analog front end). The results show that there is good correlation between the simulation and the data obtained from real systems.

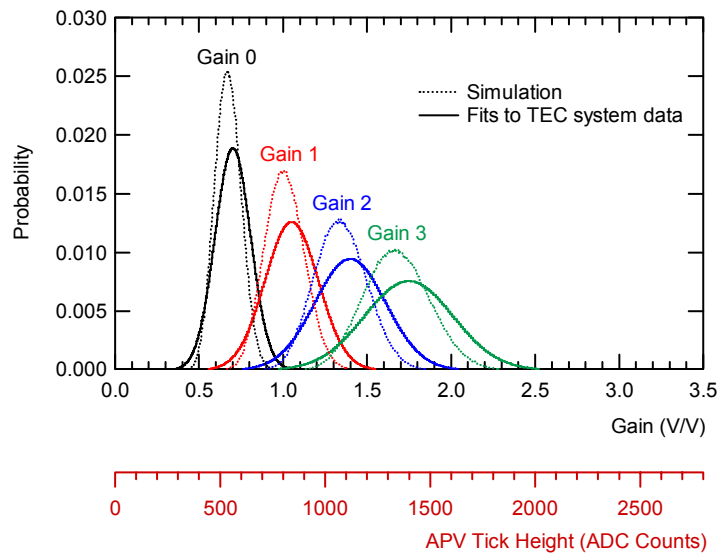


Figure 10: Comparison of the readout link gain distributions obtained by simulation and from the TEC subsystem in the June 2004 test beam.

3. Measured Gain Distribution from Deployed Optical Links

While production testing of the link's constituent components takes place at 'room temperature' at several locations, the CMS Tracker will be operated at -10°C (hybrid temperature) [1]. Hence, it is instructive to understand how the readout link gains –and hence the dynamic range– will be affected by the cold environment. The simulation based on production test data alone is not enough to quantify the optical link gain variation with temperature, since the production tests take place at room temperature.

The test beam in October 2004 at X5, CERN, presented an opportunity to study a significant number of real deployed links. The results presented in this section are from 99 operational links in the Tracker Outer Barrel CRack [12]. The cooling system of the CRack allowed the temperature dependence of gain to be studied. The gain calculation relies on data obtained by the online setup routines. It should be noted that the optical receiver's (ARx12) load resistor value was 100Ω (for the FEDs used in the test beam).

3.1 Accuracy of the Online Gain Calculation Routine

If the setup routine is to be used to draw useful conclusions about the gain spread, its accuracy must first be evaluated. The gain calculated by the online setup routine is derived from the APV header height at the output of the link. Therefore, its relationship with 'real' signals due to particles traversing the silicon detectors in the Tracker depends on sensible assumptions made about the output (and gain) of the APV. Clearly, the objective of the setup routine is to estimate the real particle gain as accurately as possible, using the most stable metric available.

The real particle gain of the readout links was measured by taking physics data on the CRack in the October 2004 test beam at CERN, X5. Histograms of the cluster signal in ADC counts at the output of each readout link in the CRack were obtained for three different runs with muons and pions, under varying conditions of temperature and APV operation mode (see [16] for more details). By performing a Landau fit for each link, the Most Probable Value (MPV) of the signal induced by a particle traversing the detectors was found. Assuming all detectors in the test system are the same¹, the value of the MPV for each link will depend on the readout system's gain. In order to have a standardized metric that is independent of the type of detector, all gains are calculated with reference to the signal size produced by a minimum ionizing particle (MIP) traversing the silicon detectors perpendicularly. This is referred to as 'MIP gain' in this document.

Figure 11 is a comparison plot of the gain calculated using the MIP signal size against the gain calculated from the setup routine using APV ticks, for one of the physics runs. The error bars denote estimated calculation error for each method. The MIP gain error was derived by the error on the Landau fit, while the setup routine error was set to a constant $\pm 5\%$ ². The plot shows very good correlation between the MIP gain and setup routine gain and hence the accuracy of the setup routine gain calculation is deemed satisfactory. A certain amount of offset can be expected when compared to the 'real' MIP gain, due to the fact that the APV uses a separate current reference circuit for the digital header (from which the setup routine extracts the gain). Hence, the analog and digital parts of the APV output are affected differently by operating conditions (namely temperature and APV parameter settings), and one cannot expect perfect correlation between the setup routine and MIP gain in all cases. Results in [16] show that this offset should be no more than $\sim 10\%$ for relevant temperature ranges (-10°C to 25°C air temperature). This is relatively small compared to the granularity of the AOH gain settings (50% steps). Hence, when equalizing the gain of the links throughout the Tracker, the gain error induced by the setup calculation should have a negligible effect.

¹ In terms of the factors that affect the signal size at the output of the sensor's electronics (i.e. the amount of charge collected resulting from incident particles). In practice these will be different from sensor to sensor, though the effect should be negligible compared to the link gain variation.

² This is only an estimate, based on past experience with the setup routine method. The error will be dependent on the exact gain calculation algorithm implemented in the system.

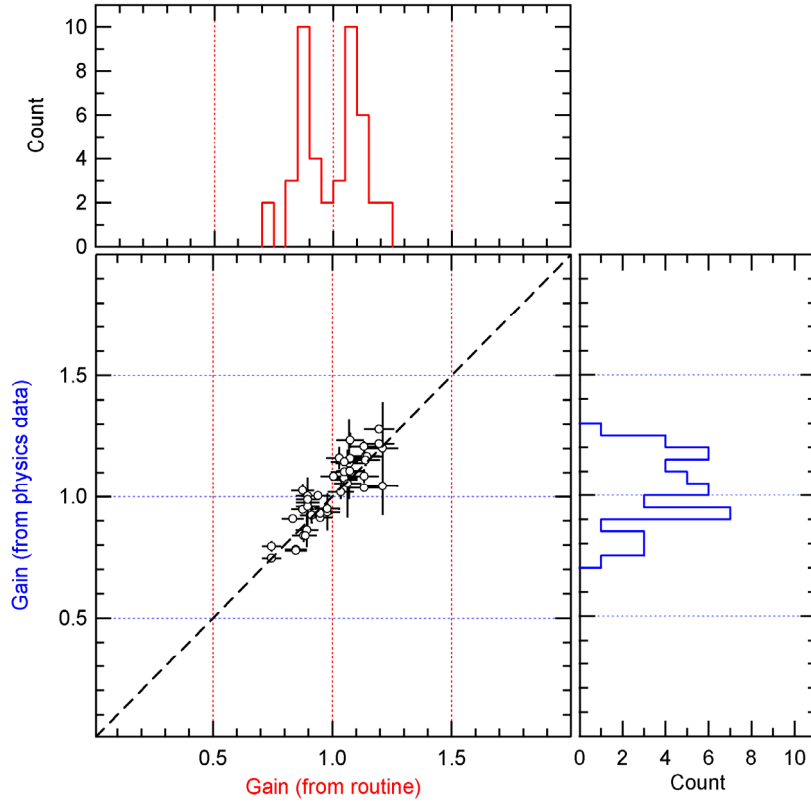


Figure 11: Comparison of gains calculated from physics data and the automated setup routine for one of the runs analyzed (muons, $T_{\text{air}}=-12^{\circ}\text{C}$, peak mode).

Finally, the setup routine gain calculation was purposely designed to depend on a link input quantity (the APV digital header height) that is a constant regardless of other front-end detector hybrid settings (i.e. APV parameters that affect the chip's gain). It follows that the correlation of the gain values calculated by the physics data and the setup routine then depends on the particular conditions and parameters chosen by the users. The setup routine therefore provides a good estimate of the gain; after having setup the optical links with the automated routines, users can obtain signal size histograms from real physics data to fine-tune the gains as required.

3.2 *Optical Link Gain in the CRack as a Function of Temperature*

The air temperature in the CRack was used for this study, since it is approximately a constant for all modules, and should track proportionally with the variation of hybrid temperatures. The gain distributions obtained from four setup runs of the 99 operational CRack optical links are shown in Figure 12. In each plot the dotted line represents the distribution resulting from setting all links to AOH gain setting 0. The

solid line is the distribution obtained when attempting to equalize all links to the same target value of $0.8V/V^1$ (the target is indicated by the dashed line on the x-axis).

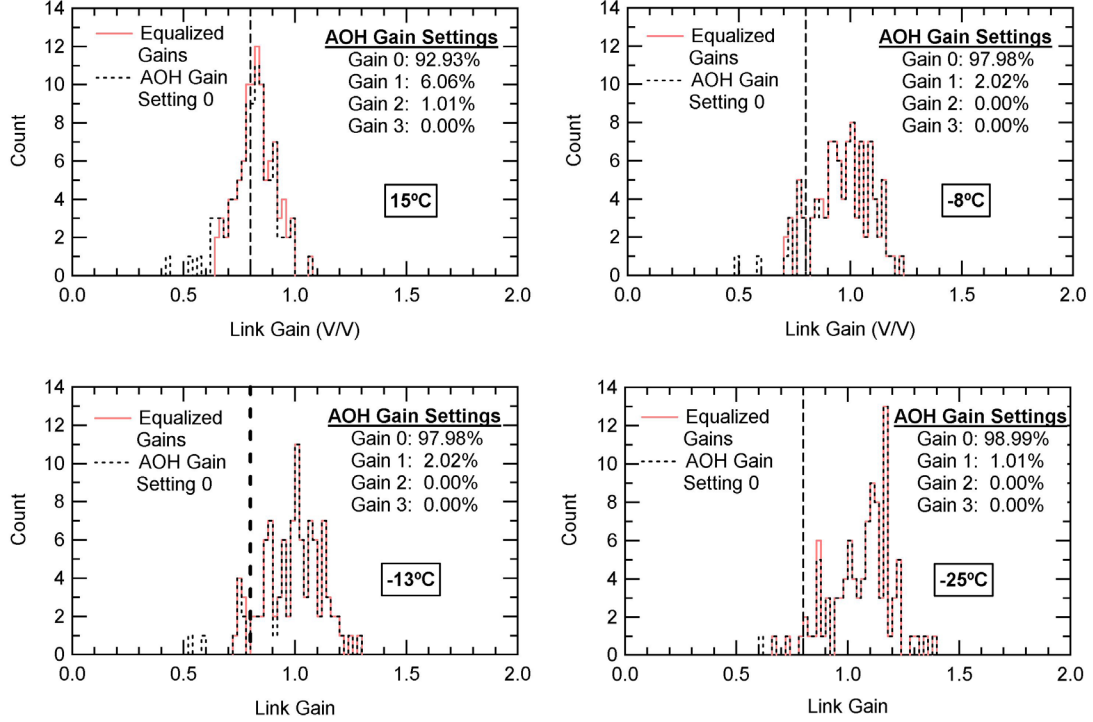


Figure 12: Readout link gain spreads for the 99 CRack links in the October 2004 test beam, for four different temperatures

In order to verify that the CRack's AOH temperatures change in proportion to the system's air temperature, the average laser bias point was determined for each run. The bias point refers to the optimum operating point of the AOH, as determined by the setup runs². The bias point is proportional to the laser threshold. The threshold's dependence on relative temperature, ΔT , is given by [17]:

$$I_{th} = I_{th}(0) \cdot \exp(\Delta T / T_0) \quad (4)$$

T_0 and $I_{th}(0)$ are known as the characteristic temperature and current. Taking the natural logarithm:

$$\ln(I_{th}) = \ln(I_{th}(0)) + \Delta T / T_0 \quad (5)$$

¹ The target gain of 0.8 is the specification for the optical readout links of the CMS Tracker.

² The AOH provides a bias current for the lasers, selectable in I^2C steps, worth $\sim 0.45\text{mA}$ each. The 'optimum' point is the first I^2C setting after the laser threshold (i.e. where lasing starts).

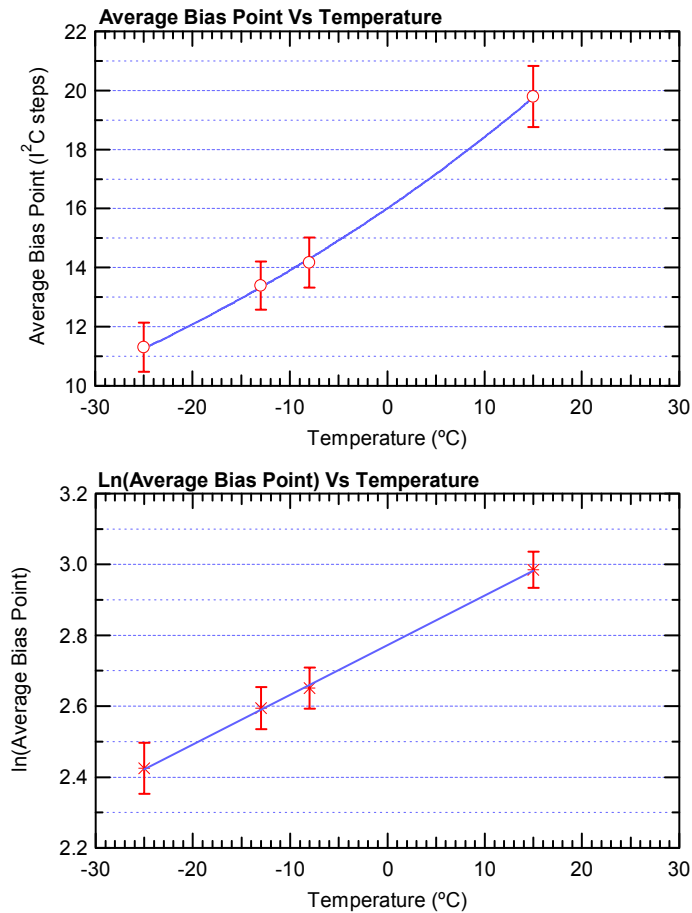


Figure 13: Average laser bias point (in I²C steps) versus temperature (top) and ln(average laser bias point) versus temperature (bottom). The error bars denote +/- 1 standard deviation from the mean.

Hence the natural logarithm of the threshold current (and therefore the bias point) varies proportionally to laser temperature. Figure 13 shows the average bias point (per CRack setup run, for the 99 links) versus air temperature (top), as well as the natural logarithm of the average bias point versus air temperature (bottom). Clearly the two plots follow the relationships of equations (4) and (5). This implies that the temperature of the lasers on the AOHs in the CRack was indeed proportional to the air temperature of the system, giving confidence in the results obtained in this section.

Figure 14 shows the gain-temperature correlation plot obtained from the four setup runs analyzed. Each point on the plot corresponds to the mean gain of all 99 links for that particular run (only AOH gain setting 0 is considered for calculating the mean).

There is an obvious trend of increasing gain with lower temperature, from the above results. The spread of the gain distribution also seems to become larger. Even at 15°C and with all links set to AOH gain setting 0, the gains of the links are on the high end. As a consequence, when attempting to equalize to 0.8V/V, the vast majority of the links (93%) have to be set to the lowest gain setting in order to be closest to the target

gain. Indeed, the mean gain is 0.81V/V at this temperature, allowing very little flexibility for compensating high gain links. As the temperature is lowered the problem of high gain gets even worse, as can be seen in Figure 12. For temperatures below 15°C the mean gain of the CRack links is over 0.8. With a load resistor of 100Ω, high gain links cannot be compensated for, resulting in large gain spread in the system.

By fitting a straight line through the points in Figure 14 the average gain increase with temperature is found to be $-0.0064 \text{ } ^\circ\text{C}^{-1}$. For a temperature change of +25 to -10°C ($\Delta T=35^\circ\text{C}$) the gain increases by ~30%. The corresponding change in APV tick height is from ~595 to 774 ADC counts, at gain setting 0. This result can be compared to previous measurements made on the individual front-end components of the readout links that will also be cooled. While the temperature dependence of laser efficiency is not necessarily linear, it has been shown that the efficiency generally increases with temperature. In [18] the Mitsubishi laser transmitters showed an average efficiency increase of 0.22%/°C. For a $\Delta T=35 \text{ } ^\circ\text{C}$, this translates to a gain increase of ~8%. The APV25 digital header changes by about ~8-9% when cooled by the same amount [14]. Finally, there are no data regarding the gain of the APVMUX [1] and LLD chips. However, one would also expect an increase in gain with lower temperature. Hence, the 30% change obtained from the CRack test beam results seems to be reasonable for the full readout chain gain.

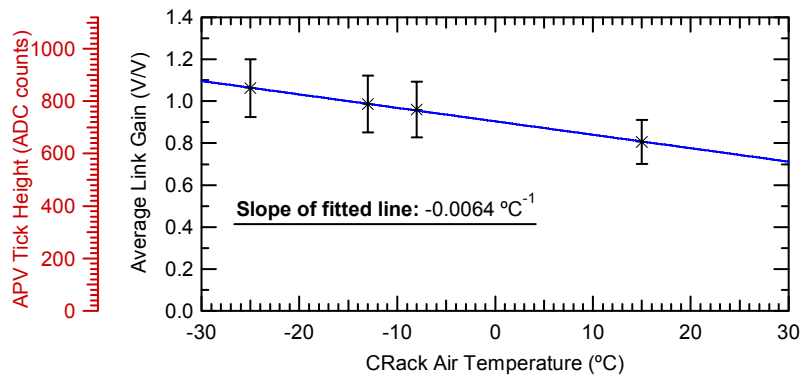


Figure 14: Average link gain vs CRack air temperature for all four setup runs analyzed. The error bars denote +/- 1 standard deviation from the mean.

4. Predicting the Final Gain Spread in the CMS Tracker Optical Links at the Nominal Operating Temperature

Production tests occur only at room temperature, and hence the effect of temperature on the individual component gains is unknown. The temperature dependence of the *overall* link gain was investigated in the previous section, using data from deployed links in the CRack. From Figure 14, the temperature change from +25°C to -10°C corresponds to an average link gain increase of ~30%. This increase was incorporated into the Monte Carlo simulation in order to obtain the best estimate of gain spread that can be expected in the final system during operating conditions.

It should be noted that, while laser transmitter efficiency generally shows an increase in gain with lower temperature, this varies from device to device and is due to the unpredictable variation in laser-fiber coupling efficiency [18]. Hence operation at different temperatures implies a varying *spread* of laser transmitter slope efficiency, and therefore of the aggregate link gain. Since there are no significant statistics on this change with temperature, the effect of temperature on the spread of the efficiency has been ignored in this study. Instead, the laser efficiency (and the overall link gain) is assumed to vary in direct proportion to the temperature (i.e. this study uses the average gain increase. This should not affect the accuracy of the final results, since the uncertainty in the spread is lower than the granularity of the AOH gain settings, and is effectively masked. This has been confirmed in [16] where low temperature measurements on deployed links are presented.

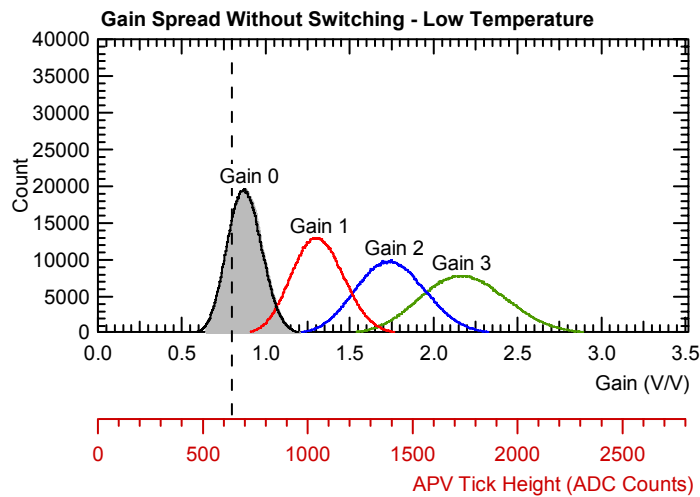


Figure 15: Showing the ‘single gain’ spread distributions predicted by simulation without switching of the LLD, at -10°C . The shaded area shows the distribution resulting after equalization using the 4 available gain settings.

Figure 15 shows the non-equalized, single-gain distributions obtained via simulation for low temperature. The mean of the gain 0 distribution is above the target value of 0.8V/V . Virtually all links would have to be set to AOH gain setting 0 when attempting to use equalization. This is illustrated in Figure 16 which also indicates the percentage of links set to each gain setting. It is also noteworthy that the total spread of the equalized distribution is higher, with the lowest gain at 0.64 and the highest at 1.32V/V . The low end is the same as in the room temperature case, while the high end corresponds to the tail of the gain 0 distribution (i.e. high gain links for which there is no lower AOH gain setting).

The higher gains (with respect to the design specification) observed can be attributed to the fact that the system was designed assuming uniform spreads in the connector losses, within their specifications ($0\text{-}0.6\text{dB}$ for the MU and $0\text{-}1.2\text{dB}$ for the MFS connectors). In reality, the insertion losses of the connectors are far better (Figure 3). In addition, the LLD transconductance is on the high end of its specification (roughly 7% higher than the nominal).

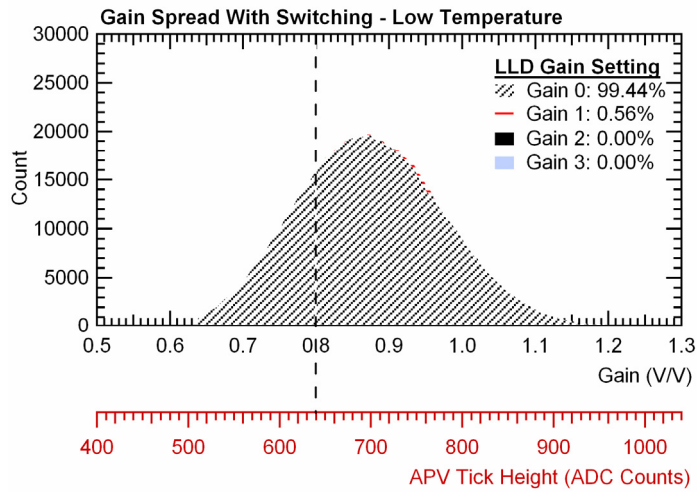


Figure 16: Equalized link gain distribution at -10°C obtained by switching of the LLD, showing the contributions from each gain setting.

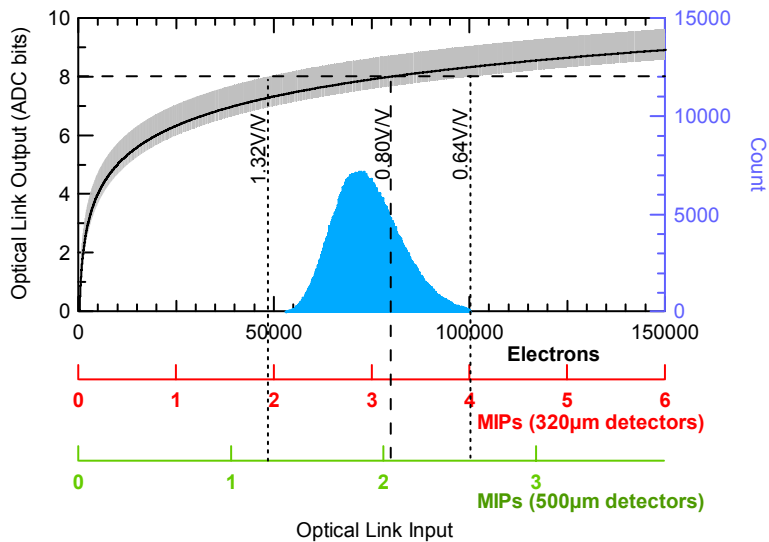


Figure 17: Showing Optical Link Output vs Input in ADC bits (left axis) for -10°C . The histogram (right axis) shows the spread in dynamic range.

The results clearly show that the gain of the optical links is too high, for low temperature and a load resistor value of 100Ω . This is not an ideal situation, and the ability to equalize the optical link gains is completely lost. The effect on the dynamic range is illustrated in Figure 17. Due to the inability to equalize the gains, the dynamic range spread is significantly increased when compared to room temperature, with the low-end of the distribution tail at $\sim 48\,500$ electrons/8bits (~ 1.9 MIPs/8bits for thin detectors) and the high-end at $\sim 100\,000$ electrons/8bits (4 MIPs/8bits for thin detectors). For thick detectors, the corresponding distribution ranges from 1.2 to 2.6 MIPs/8bits.

4.1 Gain Compensation: Changing the ARx12 Load Resistor

While, the optoelectronic receiver's (ARx12) load resistor value will be fixed for the duration of the experiment, it provides a handle for adjustment of the overall link gain before the value is frozen. Using the Monte Carlo simulation, the effect of changing the load resistor can be observed. The new value must be such that it allows recovery of the dynamic range lost due to temperature effects (~30%). In addition, even at room temperature the vast majority of links have to be operated at one of the extreme AOH gain settings (setting 0). This does not allow much equalization flexibility, and hence it is desirable to further adjust the gain so that AOH setting 1 is the most common setting. The resistor value that achieves both of the above objectives was found via simulation to be 62Ω . The single-gain and equalized distributions are shown in Figure 18 and Figure 19, while Figure 20 shows the dynamic range spread that can be expected with a load resistor of 62Ω . The results show that the ability to equalize the gains at the nominal Tracker operating temperature can be recovered with this load resistor value. The equalized gain spread lies between ~ 0.64 and $0.96V/V$, as expected. Furthermore, the most frequent AOH gain setting will be setting 1, allowing sufficient flexibility for compensation of both low and high gain links. This change in the load resistor has been implemented on the production version of the FED (version 2).

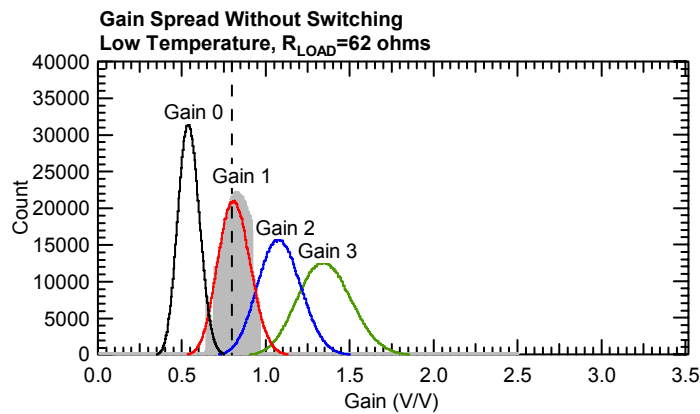


Figure 18: Showing the ‘single gain’ spread distributions predicted by simulation without switching of the LLD, at -10°C and an ARx12 load resistor of 62Ω . The shaded area shows the distribution resulting after equalization using the four available gain settings.

Table 1 gives the simulated limits on the APV tick heights that will be observed after equalization at various temperatures, with a load resistor of 62Ω . Results are shown for the full range of data, as well as for 98% of the links.

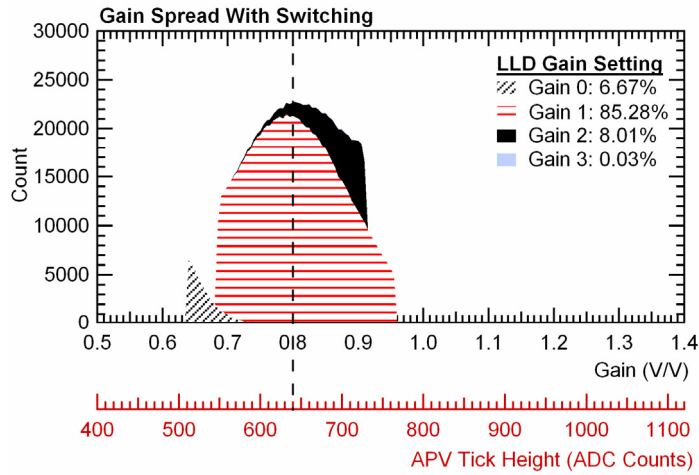


Figure 19: Equalized link gain distribution at -10°C with switching of the LLD and an ARx12 load resistor of 62Ω , showing the contributions from each gain setting.

The expected mean, minimum and maximum APV tick heights after equalizing with the AOH gain settings are given for various air temperatures from $+25$ to -20°C . The corresponding usage of AOH gain settings in the equalization process is also shown in Table 1. The final column indicates the percentage gain increase that is expected for the non-equalized case (i.e. the average increase of link gain that would be expected if only a single AOH gain setting is used). It should be noted that the air temperature/gain relationship is only exactly valid for the CRack system, though it may be very similar to other systems. In any case, the range of temperature (and corresponding gain) explored shows that equalization is possible in every case, and that it will result in the gain range calculated above.

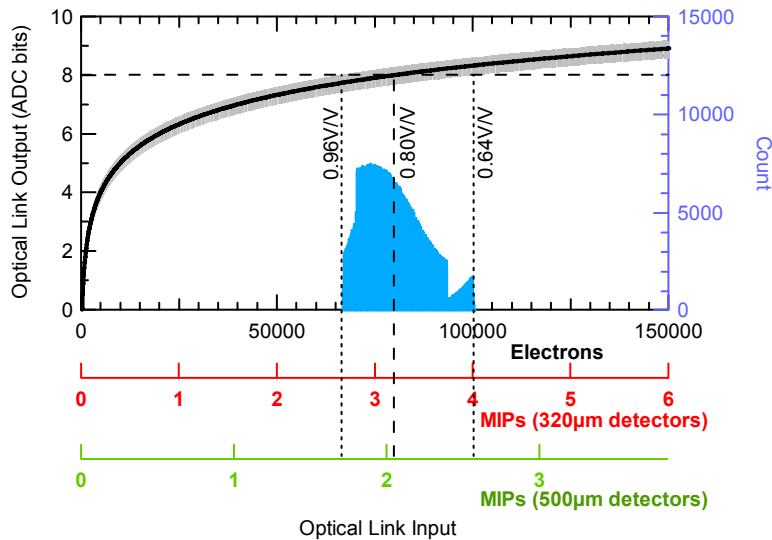


Figure 20: Showing Optical Link Output vs Input in ADC bits (left axis) for -10°C an ARx12 load resistor of 62Ω . The histogram (right axis) shows the spread in dynamic range.

Table 1: Simulation results for various temperatures.

Air Temperature (°C)	Tick Height after Equalization (ADC Counts)				AOH Gain Settings Used (%)				Average Non-Switched Gain Change (%)
		Min	Mean	Max	Gain 0	Gain 1	Gain 2	Gain 3	
25	Full Range	472	640	752	0	20	70	10	0.0
	98%	551	640	728					
	Gain (Full Range)	0.590	0.800	0.940					
20	Full Range	492	639	768	0	33	62	5	4.3
	98%	550	639	729					
	Gain (Full Range)	0.615	0.799	0.960					
15	Full Range	508	637	772	0	46	52	2	8.6
	98%	550	637	730					
	Gain (Full Range)	0.635	0.796	0.965					
10	Full Range	508	635	772	0	59	40	1	12.9
	98%	550	635	731					
	Gain (Full Range)	0.635	0.793	0.965					
5	Full Range	508	636	772	0	70	29	1	17.2
	98%	549	636	739					
	Gain (Full Range)	0.635	0.795	0.965					
0	Full Range	508	640	772	1	79	20	0	21.5
	98%	535	640	752					
	Gain (Full Range)	0.635	0.800	0.965					
-5	Full Range	508	644	772	3	84	13	0	25.9
	98%	520	644	759					
	Gain (Full Range)	0.635	0.805	0.965					
-10	Full Range	508	649	772	7	85	8	0	30.2
	98%	517	649	762					
	Gain (Full Range)	0.635	0.811	0.965					
-15	Full Range	508	651	772	11	84	5	0	34.5
	98%	515	651	764					
	Gain (Full Range)	0.635	0.814	0.965					
-20	Full Range	508	650	772	18	79	3	0	38.8
	98%	514	650	765					
	Gain (Full Range)	0.635	0.813	0.965					

4.2 Errors and Limitations

The relationship between gain and temperature was explored using data from real systems with a significant number of readout links deployed. The automated setup routines were used for extracting the gains of the links and their accuracy was verified using real physics data (section 3.1). While the results show good correlation between the ‘real’ particle gain in the physics runs and the gain calculated by the routine, there is some remaining uncertainty. As far as the setup routine gain calculation is concerned, (small) disagreement between runs was observed even in cases where the (reported) air temperatures were the same. The discrepancy could be due to the temperatures on the AOHs being different between physics runs with the same reported air temperatures.

Certainly the most obvious source of error regarding the conclusions that can be drawn when comparing

different systems is the uncertainty of the front-end temperature. The CRack air temperature was consistently used in all measurements, but this does not necessarily coincide exactly with the hybrid or sensor temperatures. The results rely on the fact that the *relative change* in the temperature of the electronics is similar to that of the air temperature. We have shown that this is the case in the results of section 3.2. Clearly, the conclusions reached in this document are exactly valid only for the CRack, but are expected to be similar for all sub-systems in the final CMS Tracker.

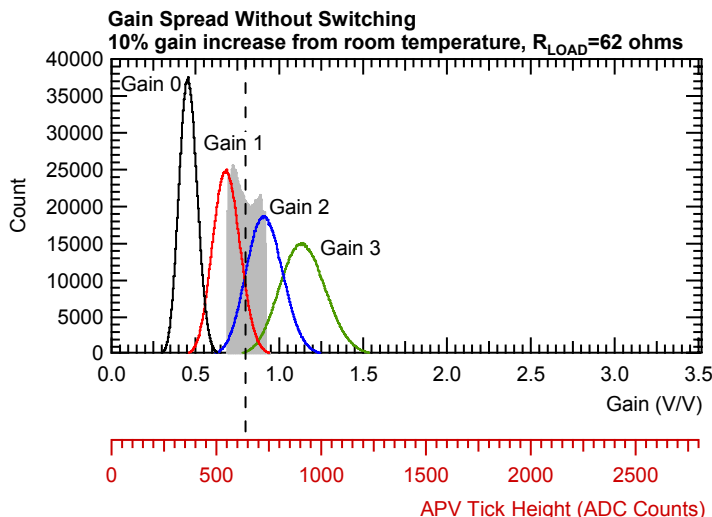


Figure 21: Illustrating the effect on the single-gain and equalized (shaded histogram) distributions of a 10% gain increase (relative to the room temperature simulation and with a load resistor of 62Ω).

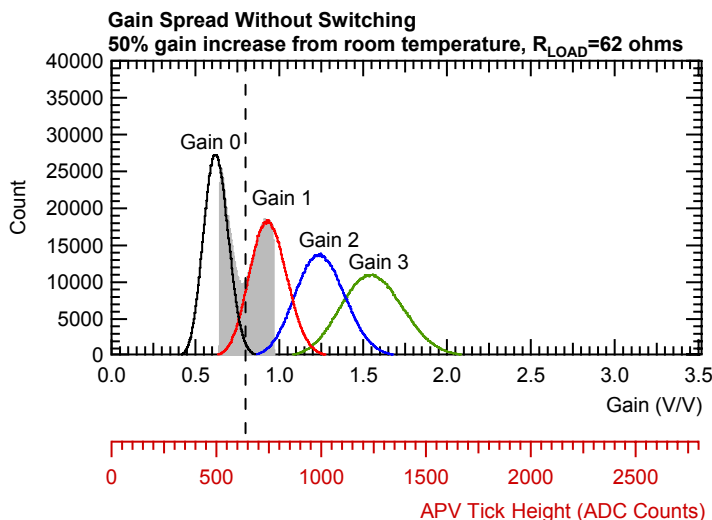


Figure 22: Illustrating the effect on the single-gain and equalized (shaded histogram) distributions of a 50% gain increase (relative to the room temperature simulation and with a load resistor of 62Ω).

The effect that the above errors have on the conclusions drawn by this study can be easily seen using the Monte Carlo simulation of the link gain. Recognizing that the choice of load resistor value required to

recover lost dynamic range hinges on the temperature-gain dependency result, it is possible to simulate what would happen to the link gains (with 62Ω load resistors) if the *assumed* gain change with temperature is off by a large amount. Figure 21 shows the single-gain distributions obtained via simulation, assuming the average gain increase at nominal Tracker operating temperature is only 10% compared to room temperature. Figure 22 shows the results assuming a gain increase of 50%. In both cases, the single-gain distributions are such that, with a target gain of $0.8V/V$, the link gains can be equalized within the 0.64 to $0.96V/V$ window. The results give confidence in the choice of load resistor value, since they show that even if the gain-temperature relationship has been calculated wrongly, gain equalization (and hence the dynamic range spread) will not be affected.

The physics runs used in evaluation of the setup routine accuracy were limited in the statistics (i.e. number of particles hitting the detectors). In order to draw a useful conclusion regarding the correlation between the gain calculated by the setup routine and that from physics data, one should have sufficient readout links to compare. Since most detectors in the CRack were not in the beam, there were fewer readout links that could be used in the first place. In addition, a decision had to be made about the minimum number of entries a cluster size histogram should have to obtain a decent Landau fit. This had to be chosen low enough so that enough links could be included in the calculations (20-40 links), but high enough to obtain a relatively low error on the fit. Therefore the gains calculated from the physics runs should be used cautiously, in order to make a rough comparison with the gains obtained by the setup routine.

Finally, the actual spread of the single-gain distributions obtained via simulation is expected to be larger in a real system. This is due to the components not simulated (notably the APV and APVMUX chips, and the analog front end of the FED). However, with the change in load resistor implemented, the spread on each single-gain distribution would have to roughly double (compared with that predicted by the simulation) before the equalized spread can no longer be contained between the 0.64 - $0.96V/V$ window. Therefore the conclusions drawn by the simulation are still most likely to be exact, despite the slightly optimistic spread in the single-gain distributions.

5. Summary and Conclusions

The gain spread that can be expected in the CMS Tracker analog optical readout links has been studied by means of a Monte Carlo simulation relying on production data. The dependence on temperature of optical link gain was determined by measurements made on the TOB CRack in the October 2004 test beam at X5, CERN. A linear relationship between gain and temperature was assumed and incorporated into the Monte Carlo simulation, in order to predict the gain spread at the nominal CMS Tracker operating temperature of -10°C .

The results at low temperature showed that the gains of the readout links calculated by simulation using real production data were too high, and the ability to use the AOH gain switch for equalization near the target gain value was completely lost. Consequently, the spread in dynamic range became unacceptably

high. The simulation was used to determine the value of optoelectronic receiver load resistor that was needed in order to lower the gains and hence recover the lost dynamic range of the system. The new value (62Ω) was implemented in the production version of the FED board.

An analysis of potential errors concerning the temperature dependence of optical link gain was introduced. It has been shown that even with a large error in the expected gain change at low temperature, the new load resistor value will ensure that all gains in the Tracker's readout optical links will lie within the 0.64-0.96V/V window after equalization. Hence, once equalized, the spread in dynamic range of the final readout system will be from 2.7 (1.7) to 4 (3.6) MIPs/8bits for thin (thick) detectors (assuming that the 8 LSBs of the data captured at the FED's ADC are retained). The corresponding spread in APV tick heights is 512 to 768 ADC counts.

References

- [1] "CMS Tracker Project Technical Design Report," CERN LHCC 98-61998, and Addendum, CERN/LHCC 2000-016, February 2000, April.
- [2] M. Raymond, *et al.*, "The APV25 0.25 μm CMOS readout chip for the CMS tracker," *Nuclear Science Symposium Conference Record, 2000 IEEE*, vol. 2, pp. 9/113-9/118, 2000.
- [3] John Coughlan, *et al.*, "CMS Tracker Front-End Driver," *9th Workshop on Electronics for LHC Experiments*, vol. CERN/LHCC/2003-006, pp. 255-259, 2003.
- [4] G. Cervelli, *et al.*, "A radiation tolerant laser driver array for optical transmission in the LHC experiments," *7th Workshop on Electronics for LHC Experiments*, vol. CERN/LHCC/2001-005, pp. 155-159, 2001.
- [5] M. Friedl, "Analog optohybrids for the readout of the CMS silicon tracker," *Nuclear Instruments and Methods in Physics Research A 518*, pp. 515-518, 2004.
- [6] Raquel Macias, *et al.*, "Advance Validation of Radiation Hardness and Reliability of Lasers for CMS Optical Links," *IEEE Trans. Nucl. Sci.*, vol. 52, pp. 1488-1496, 2005.
- [7] J. Troska, *et al.*, "Radiation effects in commercial off-the-shelf single-mode optical fibres," *Proceedings of the SPIE*, vol. 3440, 1998.
- [8] Francois Vasey, *et al.*, "A 12-Channel Analog Optical-Receiver Module," *Journal of Lightwave Technology*, vol. 23, pp. 4270-4276, 2005.
- [9] Thomas Bauer, "A model for the CMS Tracker analog optical link," CMS Note 2000/056, 2000.
- [10] S. Dris, *et al.*, "Predicting the in-system performance of the CMS tracker analog readout optical links," *10th Workshop on Electronics for LHC Experiments*, vol. CERN/LHCC/2004-030, pp. 164-168, 2004.
- [11] Katja Klein, *et al.*, "Design and test beam performance of substructures of the CMS tracker end caps," CMS NOTE 2005/025, December 5 2005.
- [12] T. Lampen, *et al.*, "Alignment of the Cosmic Rack with the Hits and Impact Points Algorithm," CMS NOTE 2006/006, 2006.
- [13] M. Raymond, *et al.*, "Final Results from the APV25 Production Wafer Testing," *11th Workshop on Electronics for LHC Experiments*, vol. CERN/LHCC/2005-038, pp. 453-457, 2005.
- [14] M. Raymond (private communication), 2004.
- [15] S. Eidelman, *et al.*, "The review of particle physics," *Physics Letters B592*, vol. 1, 2004.
- [16] S. Dris, "Performance of CMS Tracker Optical Links and Future Upgrade using Bandwidth Efficient Digital Modulation," vol. PhD. London: Imperial College, 2006.
- [17] J. I. Pankove, "Temperature Dependence of Emission Efficiency and Lasing Threshold in Laser Diodes," *IEEE J. Quantum Electron.*, vol. QE-4, pp. 119-122, 1968.
- [18] Raquel Macias, "Laser threshold current and efficiency at temperatures between -20°C and $+20^{\circ}\text{C}$," EDMS document CMS-TK-TR-0036, 2003.